Plaque Distribution of Basilar Artery Fenestration by 3D High-Resolution MR Vessel Wall Imaging

Lei Liu, MD[1]⑩, Xue-Bin Zhang, MD[2]⑩, Shuo Lu, MD[1]⑩,
Zun-Jing Liu, MD[1]⑩, and Xian-Jin Zhu, MD[2]⑩

Abstract

The association between fenestrations and neurovascular pathology is not well defined. The morphology of vessel wall plays an important role in the development of neurovascular pathology. We sought to explore the plaque distribution around basilar artery fenestration (BAF) by three-dimensional high-resolution MR vessel wall imaging (3D HRMRI). Patients with BAF on 3D HRMRI images were enrolled. All cross-sectional slices of basilar arteries were assessed and categorized based on the location of fenestration as proximal segment, in-bifurcation segment, and distal segment. Furthermore, plaques in the in-bifurcation segment were classified according to their orientation being centered on the lateral, interior, dorsal, or ventral wall of the vessel. In all, 12 cases with BAF involving 661 cross-sectional image slices in entire basilar arteries were included. Plaques were found in 190 image slices, with the distribution of 41 slices in the proximal segment, 144 slices in the in-bifurcation segment and 67 slices in the distal segment. Plaques were found more frequently in the proximal and in-bifurcation segments than in the distal segment ($P < 0.001$), but there was no statistical difference between the proximal and in-bifurcation segment ($P = 0.11$). In the in-bifurcation segment, plaques were more frequently located at the lateral (50.0%) than other interior (16.0%), dorsal (21.0%), and ventral (13.0%) wall ($P < 0.001$).Plaques of BAF tend to locate in the proximal and in-bifurcation segments, especially at the lateral wall of the in-bifurcation segment.

Introduction

Arterial fenestration is a rare but well-known vascular variation that is defined as a localized duplication of an artery, with a divided arterial lumen including division of the endothelium and tunica media, and, in some instances, the adventitia[1]. The length of the fenestration ranges from 1 mm to several centimeters; most are <5 mm[2,3]. The location varies from the anterior cerebral artery to the vertebrobasilar system, and the most frequent sites are anterior communicating region and basilar artery[4,5].

Because of the intrinsic anatomic difference between fenestration and conventional artery, interest is focused on the relationship between fenestration and neurovascular pathology. The association of fenestration with aneurysm[6,7] and ischemic stroke[8–10] has been suggested in case reports or small case series, though the exact relationship is not well defined. As we know, vessel wall morphology plays an important role in the development of neurovascular pathology. It is important to observe the vessel wall morphology around fenestration in order to understand the relationship between fenestration and neurovascular pathology[11].

Conventional non-invasive imaging techniques, including computed tomography angiogram (CTA) and magnetic resonance angiography (MRA), are widely used in detecting fenestrations and providing information about location and adjacent structures as well as the arterial lumen morphology.

[1] Department of Neurology, China-Japan Friendship Hospital, Beijing, China
[2] Department of Radiology, China-Japan Friendship Hospital, Beijing, China

Corresponding Authors:
Zun-Jing Liu, Department of Neurology, China-Japan Friendship Hospital, No.2 Yinghuayuan Dongjie, Beijing, China.
Email: liuzunjing@163.com
Xian-Jin Zhu, Department of Radiology, China-Japan Friendship Hospital, No.2 Yinghuayuan Dongjie, Beijing, China.
Email: xianjinzhu@yeah.net

But they do not provide high quality information regarding vessel wall morphology[12,13]. Recently, high-resolution magnetic resonance imaging (HRMRI) has emerged as an effective tool for assessing the morphological features of the intracranial artery wall, including plaques not visualized by MRA or CTA, plaque size, percent plaque burden, and remodeling pattern of intracranial atherosclerosis[14,15]. A new three-dimensional (3D) black blood technique called volumetric isotropic turbo spin echo acquisition (VISTA) sequences has the advantages of high isotropic resolution and multiple planar reconstruction, which helps assess the wall characteristics of tortuous intracranial arteries more accurately[16].

In this study, we analyzed the vessel wall around basilar artery fenestration (BAF) by 3D HRMRI of vessel walls.

Materials and Methods

Patients

The Institutional Ethics Committees of China-Japan Friendship Hospital approved this study (No. 2014-23), and all patients signed a written consent before each 3D HRMRI examination. Between April 2014 and March 2017, 3D HRMRI was performed in 543 cases (383 males; 160 females) for various indications. Patients with BAF were included in this study, except those confirmed or suspected of nonatherosclerotic vasculopathy, such as arteritis, moyamoya disease, and dissection. The following characteristics were recorded in a database: examination date, patient name and sex, date of birth, risk factors including hypertension, hyperlipidemia, diabetes mellitus, smoking, and obesity[17,18].

HRMR Imaging Protocol

A 3 T MR scanner (Ingenia; Philips Healthcare, Best, The Netherlands) with a 15-channel phased-array head coil was used in this study. 3D-HRMRI images were acquired in a traversal plane to cover the major intracranial arteries identified on the time of flight (TOF) MRA. Imaging parameters were as follows: repetition time/echo time = 1300 ms/36 ms, field of view = $140 \times 200 \times 105$ mm^3, matrix = $280 \times 332 \times 210$, number of excitation = 2. Acquisition voxel volume was $0.5 \times 0.6 \times 0.5$ mm^3 and reconstruction voxel volume was $0.5 \times 0.5 \times 0.5$ mm^3. The short axial cross-sections were constructed automatically with 0.5 mm slice thickness.

Basilar Artery Fenestration Assessment

Images were independently analyzed on a digital picture archiving and communication (PACS) workstation by two experienced doctors (a neurologist and a radiologist) using visual inspection. The differences between two observers were solved by consensus. Image quality was assessed using a previously developed 4-point scale (1 = poor quality, 2 = adequate quality, 3 = good quality, and 4 = excellent)[19].

Images were assessed on all cross-sectional image slices with a score of ≥ 2. A plaque was identified if there was
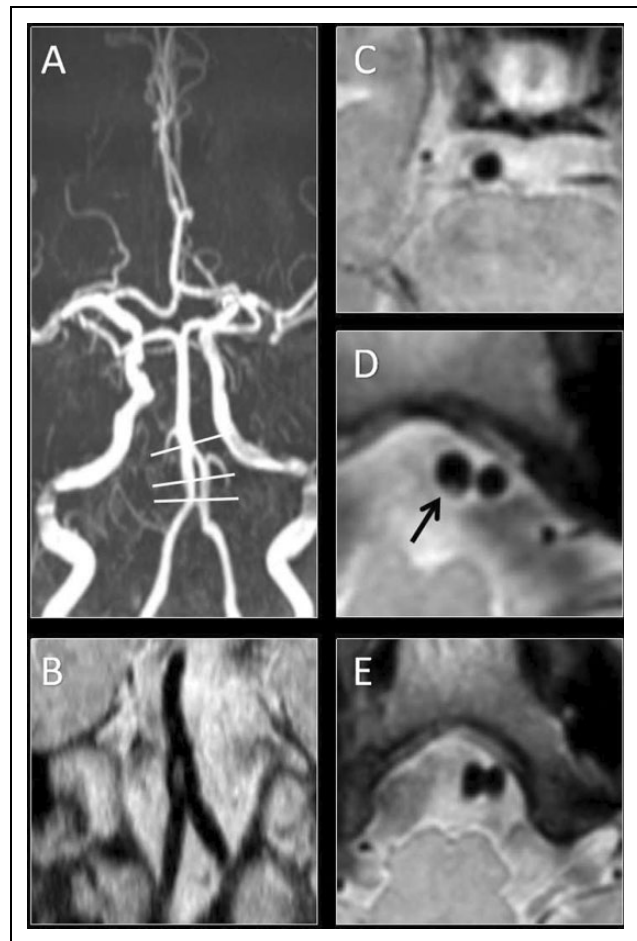

Fig 1. Images of basilar artery fenestration in MRA (A) and HRMRI (B–E). The coronal (B) images showed the structure of fenestration. Cross-sectional image were obtained in the proximal (E), in-bifurcation (D), and distal segment (C) of BA, and plaque was found in the in-bifurcation segment (D).

eccentric wall thickening and the thinnest part was estimated to be <50% of the thickest point by visual inspection[20]. Because obliquity artifacts for the tortuous basilar artery in the cross-sections would lead to overestimation of the true wall thickness, and mimic plaque, we angled reconstructed planes of 3D-VISTA to ensure that all the cross-sectional images were perpendicular the long axial of BA.

BA was divided into three segments according to the location of fenestration: proximal segment, in-bifurcation segment, and distal segment [Fig 1]. In the in-bifurcation segment, all cross-sections were classified into four quadrants based on their plaque orientation being centered on the lateral, interior, dorsal, or ventral side of the vessel [Fig 2A]. The adjacent vessel walls of the two bifurcated arteries were the interior side and the opposite were the lateral side. The two bifurcated arteries were analyzed independently. When the plaque was distributed between two quadrants, the quadrant with the maximal plaque thickness was chosen.
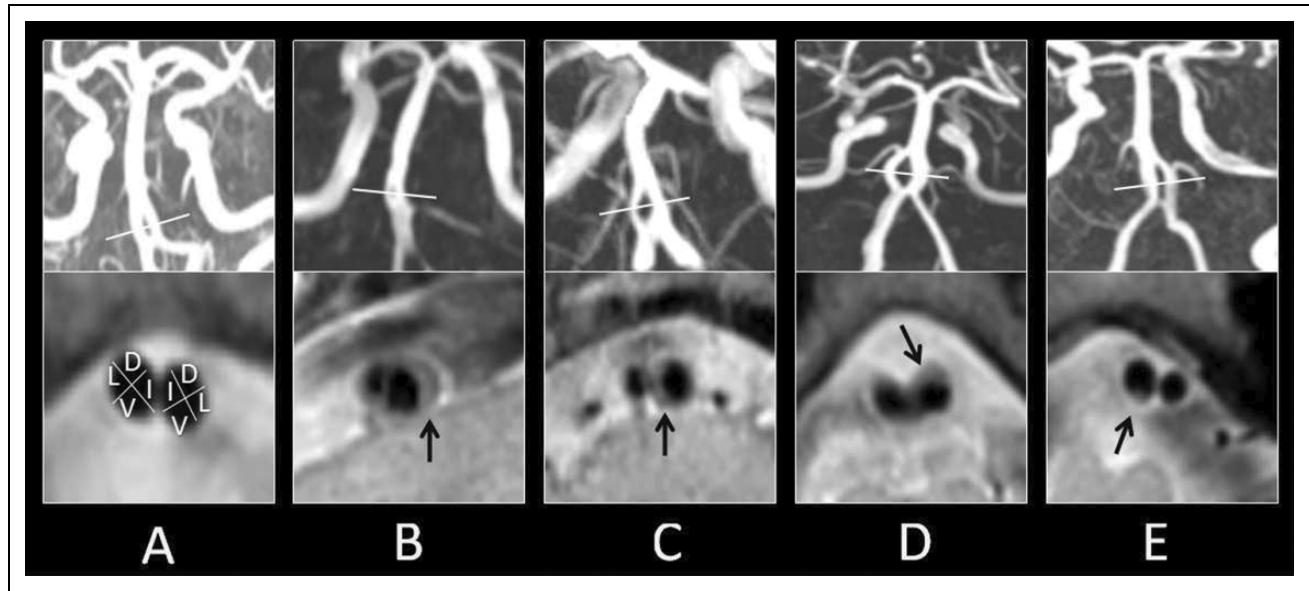
Fig 2. (A) An alignment grid to demonstrate how the adjacent vessels in each cross-section of the inbifurcation segment were divided into four quadrants (D: dorsal; L: lateral; I: interior; V: ventral). (B–E) Examples of vessel wall with plaques involving the lateral (B), interior (C), dorsal (D), and ventral (E) wall.

Statistical Analysis

Quantitative data were summarized as mean $\pm$ standard deviation (SD) and qualitative data were presented as percentage. For each patient, the percentage of plaque distribution in the whole BA and at the lateral, interior, dorsal, and ventral wall in the in-bifurcation segment were calculated separately. Plaque distribution among different segments was compared by a Chi-square test. Kruskal-Wallis test was used to compare the percentage between quadrants. SPSS 11.5 (SPSS Inc., Chicago, IL, USA) was used as the statistical analysis software. All reported P values were two-sided, and $P < 0.05$ was considered statistically significant.

Results

A total of 12 cases with BAF were included in this study. The mean age was 54 years and 11 patients were male. Among them, five patients had two atherosclerosis risk factors, four patients had three atherosclerosis risk factors, and the rest had more atherosclerosis risk factors.

A total of 661 cross-sectional image slices were obtained, all with good or excellent image quality for assessment. One patient's images were found with poor quality during the exam and repeated for good quality immediately. Plaques were found in 190 image slices, among which 41 slices were in the proximal segment, 144 slices in the in-bifurcation segment, and 67 slices in the distal segment (Table 1). Plaques were found more frequently in the proximal and in-bifurcation segments than in the distal segment ($P < 0.001$, Chi-square test). But has no statistical difference

Table 1. Plaque Distribution in Entire Basilar Arteries.

	Normal wall	Plaque	Total
Proximal segment	59 (59.0%)	41 (41.0%)	100
In-bifurcation segment	70 (44.4%)	74 (55.6%)	144
Distal segment	349 (83.5%)	69 (16.5%)	417
Total	471	190	661

between the proximal and in-bifurcation segment ($P = 0.11$, Chi-square test).

The plaque distribution of each patient in the in-bifurcation segment is outlined in Table 2. Overall, plaques were more frequently located at the lateral (50.0%), compared with the interior (16.0%), the dorsal (21.0%), and the ventral (13.0%) ($P < 0.001$, Kruskal-Wallis test). About the dominate plaques, six patients located in the lateral wall, two patients in the lateral wall, one patient in the dorsal wall, one patient in the ventral wall, and two patients were without plaque (Fig 2).

Discussion

The 3D-HRMRI technique is a new method introduced recently with high-isotropic resolution and large volume coverage for intracranial arteries. To our knowledge, we are the first to investigate the local vessel wall of BAF by 3D-HRMRI.

Our study found that plaques of BAF occurred mostly in the proximal and in-bifurcation segments. In the in-bifurcation segment, plaques were found more frequently at the lateral wall, the same as the plaque distribution of

Table 2. Individual Plaque Distribution in the in-Bifurcation Segment.

Patient	Total plaques	Lateral wall (%)	Interior wall (%)	Dorsal wall (%)	Ventral wall (%)
1	8	8 (100%)	0	0	0
2	4	0	4 (100%)	0	0
3	6	6 (100%)	0	0	0
4	7	7 (100%)	0	0	0
5	9	0	9 (100%)	0	0
6	0	0	0	0	0
7	0	0	0	0	0
8	4	4 (100%)	0	0	0
9	7	2 (28.6%)	0	0	5 (71.4%)
10	12	9 (75.0%)	0	3 (25.0%)	0
11	33	4 (12.1%)	3 (9.1%)	18 (54.6%)	8 (24.2%)
12	10	10 (100%)	0	0	0
Total	100	50 (50.0%)	16 (16.0%)	21 (21.0%)	13 (13.0%)

bifurcation of the carotid artery, intracranial artery, and coronary artery. This may be due to the hemodynamic changes in the bifurcation segment[21]. According to hydromechanics theory, blood will exert force on the vessel wall during flow, including wall pressure (WP, perpendicular to the vessel wall) and wall shear stress (WSS, parallel to the vessel wall). It has been discovered that, at the branching site of blood vessels, the interior wall shows high WP and WSS, while the lateral wall showed low WP and WSS, with an irregular distribution and high pressure gradient. Low WP is not only closely related to the thickness of blood vessel walls, but also more prone to form atherosclerosis, as the atherogenic components in the blood tend to move passively from the high pressure area to the low pressure area. The more intensively the pressure changes, the more significantly these components aggregate. Meanwhile, pressure has an influence on the vascular endothelium, as unstable pressure redistributes the atherogenic components and aggregate them under the endothelium[22]. Low WSS is another important risk factor in the formation and development of atherosclerosis. Low WSS can promote the secretion of vascular injury factors and reduce the secretion of protective factors in endothelial cells, which induces endothelial cell dysfunction and endothelial cell damage. At the same time, vascular endothelial cells in low WSS regions become round and rearrange in a disorderly manner, which increases endothelial permeability. All these factors accelerate absorption of atherogenic components and the formation of atherosclerotic lesions[23].

As the hemodynamic changes, BAF may also be a risk factor for intracranial atherosclerotic plaque. Patients with BAF should pay more attention to the control of atherosclerosis risk factors such as hypertension and hyperlipidemia.

The correlation between BAF and ischemic stroke is indistinct. Cases of infarctions due to BAF have been reported[8–10], but it has not been confirmed that fenestration is an independent risk factors for ischemic stroke. As we know, perforating branches arise predominantly from the ventral wall in the basilar artery. However, we found that plaques of BAF tend to locate at the lateral wall, which supports the view that

fenestration is not a risk factor for stroke. Nevertheless, the incidence rate for stroke may increase as the plaque grows over time. Long-term follow-up is needed to estimate the relationship between BAF and stroke.

3D HRMRI is a new method to observe intracranial vascular lesions. It can provide information about the intracranial vascular wall, which is conducive to research into intracranial vascular lesions such as BAF.

This study also has some limitations. Firstly, the sample size was small and there was no control group. More patients need to be enrolled to verify the conclusions. Meanwhile, fenestrations were always at the near-end of basilar artery; more fenestrations located in the middle should be involved. Secondly, all patients enrolled in the study were accidentally found to have BAF without symptoms and all plaques were too small to analyze morphological information such as fibrous cap on the plaque surface, thrombosis, intraplaque hemorrhage, calcification, etc. More cases are needed, especially fenestrations with stenosis, and follow-up is important in order to observe changes in the vessel walls of BAF. Last, but not least, our study only analyzed the plaque distribution of BAF, but the clinical significance was not clearly defined. A follow-up study with a larger sample size will be needed to identify clinical significance.

Conclusions

3D HRMRI revealed that plaques of BAF tend to locate in the proximal and in-bifurcation segments, especially at the lateral wall of the in-bifurcation segment. BAF may also be a risk factor for intracranial plaques, but the relationship between BAF and stroke is unclear. Long-term follow-up is needed. In addition, 3D HRMRI can provide information on the intracranial vascular wall, which is conducive to research into intracranial vascular lesions.

Ethical Approval

Statement of Human and Animal Rights

Statement of Informed Consent

Declaration of Conflicting Interests

Funding

ORCID iD

Lei Liu, MD https://orcid.org/0000-0003-1331-9363
Xue-Bin Zhang, MD https://orcid.org/0000-0001-8852-6733
Shuo Lu, MD https://orcid.org/0000-0001-8610-3817
Zun-Jing Liu, MD https://orcid.org/0000-0002-7962-8217
Xian-Jin Zhu, MD https://orcid.org/0000-0002-9647-8855

References

1. Patel MA, Caplan JM, Yang W, Colby GP, Coon AL, Tamargo RJ, Huang J. Arterial fenestrations and their association with cerebral aneurysms. J Clin Neurosci. 2014;21(12):2184–2188.

2. Teal JS, Rumbaugh CL, Bergeron RT, Segall HD. Angiographic demonstration of fenestrations of the intradural intracranial arteries. Radiology. 1973;106(1):123–126.

3. Finlay HM, Canham PB. The layered fabric of cerebral artery fenestrations. Stroke. 1994;25(9):1799–1806.

4. Van Rooij SB, Van Rooij WJ, Sluzewski M, Sprengers ME. Fenestrations of intracranial arteries detected with 3D rotational angiography. AJNR Am J Neuroradiol. 2009;30(7):1347–1350.

5. Gao LY, Guo X, Zhou JJ, Zhang Q, Fu J, Chen WJ, Yang YJ. Basilar artery fenestration detected with CT angiography. Eur Radiol. 2013;23(10):2861–2867.

6. Trivelato FP, Abud DG, Nakiri GS, de Castro Afonso LH, Ulhôa AC, Manzato LB, Rezende MT. Basilar artery fenestration aneurysms: endovascular treatment strategies based on 3D morphology. Clin Neuroradiol. 2016;26(1):73–79.

7. Sogawa K, Kikuchi Y, O'uchi T, Tanaka M, Inoue T. Fenestrations of the basilar artery demonstrated on magnetic resonance angiograms: an analysis of 212 cases. Interv Neuroradiol. 2013;19(4):461–465.

8. Kloska SP, Schlegel PM, Sträter R, Niederstadt TU. Causality of pediatric brainstem infarction and basilar artery fenestration. Pediatr Neurol. 2006;35(6):436–438.

9. Gold JJ, Crawford JR. An unusual cause of pediatric stroke secondary to congenital basilar artery fenestration. Case Rep Crit Care. 2013;2013:627972.

10. Palazzo P, Ruff M, Lyerly MJ, Alexandrov AV. Basilar artery thrombus vs. fenestration: a differential diagnostic challenge in acute ischemic stroke. J Neuroimaging. 2014;24(6):607–609.

11. Cooke DL, Stout CE, Kim WT, Kansagra AP, Yu JP, Gu A, Jewell NP, Hetts SW, Higashida RT, Dowd CF, Halbach VV. Cerebral arterial fenestrations. Interv Neuroradiol. 2014;20(3):261–274.

12. Niizuma K, Shimizu H, Takada S, Tominaga T. Middle cerebral artery plaque imaging using 3-Tesla high-resolution MRI. J Clin Neurosci. 2008;15(10):1137–1141.

13. Mandeville ET, Ayata C, Zheng Y, Mandeville JB. Translational MR neuroimaging of stroke and recovery. Transl Stroke Res. 2017;8(1):22–32.

14. Zhu XJ, Jiang WJ, Liu L, Hu LB, Wang W, Liu ZJ. Plaques of nonstenotic basilar arteries with isolated pontine infarction on three-dimensional high isotropic resolution magnetic resonance imaging. Chin Med J (Engl). 2015;128(11):1433–1437.

15. Zhu XJ, Wang W, Liu ZJ. High-resolution magnetic resonance vessel wall imaging for intracranial arterial stenosis. Chin Med J (Engl). 2016;129(11):1363–1370.

16. Zhu X, Liu L, He X, Zhang X, Hu L, Du B, Wang W, Jiang W, Liu ZJ. Wall thickening pattern in atherosclerotic basilar artery stenosis. Neurol Sci. 2016;37(2):269–276.

17. Ergul A, Hafez S, Fouda A, Fagan SC. Impact of comorbidities on acute injury and recovery in preclinical stroke research: focus on hypertension and diabetes. Transl Stroke Res. 2016;7(4):248–260.

18. Imam YZ, D'Souza A, Malik RA, Shuaib A. Secondary stroke prevention: improving diagnosis and management with newer technologies. Transl Stroke Res. 2016;7(6):458–477.

19. Zavodni AE, Wasserman BA, McClelland RL, Gomes AS, Folsom AR, Polak JF, Lima JA, Bluemke DA. Carotid artery plaque morphology and composition in relation to incident cardiovascular events: the Multi-Ethnic Study of Atherosclerosis (MESA). Radiology. 2014;271(2):381–389.

20. Xu WH, Li ML, Gao S, Ni J, Zhou LX, Yao M, Peng B, Feng F, Jin ZY, Cui LY. Plaque distribution of stenotic middle cerebral artery and its clinical relevance. Stroke. 2011;42(10):2957–2959.

21. Soulis JV, Giannoglou GD, Parcharidis GE, Louridas GE. Flow parameters in normal left coronary artery tree. implication to atherogenesis. Comput Biol Med. 2007;37(5):628–636.

22. Giannoglou GD, Soulis JV, Farmakis TM, Farmakis DM, Louridas GE. Haemodynamic factors and the important role of local low static pressure in coronary wall thickening. Int J Cardiol. 2002;86(1):27–40.

23. LaDisa JF, Olson LE, Molthen RC, Hettrick DA, Pratt PF, Hardel MD, Kersten JR, Warltier DC, Pagel PS. Alterations in wall shear stress predict sites of neointimal hyperplasia after stent implantation in rabbit iliac arteries. Am J Physiol Heart Circ Physiol. 2005;288(5):H2465–2475.